Integration and evaluation of a meander-shaped fibre-optical sensor in a GFRP leaf spring

Andreas Janetzko-Preisler[1*], *Friedrich* Wolf-Monheim[2], *Rainer* Souschek[2], *Dominik* Kaiser[3], *Ralph* Wojtczyk[4], *Athanasios* Dafnis[1], *Kai-Uwe* Schröder[1], *Wolfgang* David[2], and *Paul* Zandbergen[2]

[1] Institute of Structural Mechanics and Lightweight Design, RWTH Aachen University, Wüllnerstraße 7, 52062 Aachen, Germany
[2] Ford Research & Innovation Center Aachen, Süsterfeldstraße 200, 52074 Aachen, Germany
[3] SGL Composites GmbH, Fischerstrasse 8, 4910 Ried im Inkreis, Austria
[4] SGL Technologies GmbH, Werner-von-Siemens-Straße 18, 86405 Meitingen, Germany

Abstract. Fibre-reinforced plastics experience an increasing attention also in the non-aerospace sector. However, the detection of possible internal damage of safety-relevant components remains a challenge. In previous work, a meander-shaped sensor layout with a single fibre-optical sensor was proposed as a particularly efficient and reliable layout and its suitability was demonstrated in coupon tests. In the present work, the approach was transferred to a leaf spring made of glass fibre reinforced plastics and investigated in an extensive test campaign with a realistic test setup. The investigations show the particular suitability of the proposed meander-shaped sensor layout for simultaneous loads monitoring and structural health monitoring.

1 Introduction

Structures made of Fibre-Reinforced Plastics (FRP) are attracting more and more attention in the non-aviation sector due to their good strength-to-weight and stiffness-to-weight ratios. Forecasting component fatigue and service life, however, is a major challenge. They are subjected to a large degree of uncertainty in spite of controlled manufacturing processes. The exact onset and development of damage can only be estimated, regardless of extensive testing. Particularly difficult in this context is the fact that fatigue damage is not necessarily visible from the outside. Therefore, high and conservative safety factors are required to ensure structural integrity in service, especially for long service lives. From this, the need for Structural Health Monitoring (SHM) becomes evident. SHM describes the online monitoring of the integrity of a structure in service and thus ensures safe operation despite possible uncertainties regarding fatigue. A classification of different SHM approaches is introduced by Ritter [1] considering the level of complexity:

- Level 1 (detection) represents a system which detects solely the presence of damage.

* Corresponding author: andreas.preisler@sla.rwth-aachen.de

- Level 2 (localisation) refers to a system which is capable of determining the (rough) location of damage.
- Level 3 (assessment) defines a system which evaluates the damage in terms of size and severity.
- Level 4 (consequence) represents a system which evaluates the influence of the damage towards the structural integrity.

As the level of complexity of the monitoring response increases, logically the complexity of the required monitoring system also increases. A level 1 system would be a relatively simple system that determines the mere existence of damage from a measured value. A level 4 system, on the other hand, carries out a complete evaluation of the damage in terms of size, severity and determines the resulting residual strength and residual service life of the structure. Naturally, this requires more meaningful measurements in combination with reliable data-based or physics-based models. If the specific application allows it, physics-based models are particularly promising for evaluating the measurement signal [2]. Here, analytical and numerical models can be used in advance to determine a correlation between the measured value, the damage size and its influence on the residual strength. This correlation then forms the basis for a particularly efficient damage assessment.

When considering structures made of FRP, Fibre-Optical Sensors (FOS) are particularly promising due to their fibrous nature. They can already be integrated in the manufacturing process and thus enable measurement in the inner part of the material. In the context of SHM, two measurement methods are particularly worth mentioning. With the so-called Fibre Bragg Gratings (FBGs) [3], a measuring grid is etched into the interior of a fibre. This grating then reflects a certain wavelength, which in turn depends on the grating pitch. In the event of loading, this grating pitch is altered and the strain can thus be measured by a change in the reflected wavelength. In this way, a series of discreet measuring points along the FOS can be evaluated. The Optical Frequency Domain Reflectometry (OFDR) [4] is particularly interesting for research applications. It utilizes the natural scattering inside the fibre (the so-called Rayleigh backscatter). For this purpose, the measuring fibre is first characterised so that during operation a change in this characteristic scatter allows to evaluate the strain distribution along the FOS. This leads to a quasi-continuous strain measurement along the whole fibre, which however is prone to a certain amount of measurement noise.

In previous work, a very efficient measurement layout for a leaf spring made of Glass-Fibre-Reinforced Plastics (GFRP) was derived based on a meander-shaped design of an FOS and first investigated and validated by means of numerical investigations [2,5]. Subsequent coupon tests demonstrated the performance of the proposed measurement layout and also showed that the integrated sensor in this particular configuration has no negative influence on the static strength and stiffness [6].

In the present work, the measurement concept is validated in a demonstrator test with a leaf spring made of GFRP under realistic boundary conditions. For this purpose, several load levels are taken into account alongside test specimens with artificial delamination.

2 Monitoring concept

The monitoring concept is based on the so-called structural damage indicators [2,7-8]. These are derived by detailed consideration of the influence of the damage on the structural behaviour. By simulating the undamaged and damaged structure, measurable effects can be identified that are directly related to the damage. The monitoring of these effects can lead to damage indicators that ideally show a zero-baseline in the undamaged state. In this case, a deviation from zero can be directly attributed to the presence of damage, while the magnitude of the deviation usually correlates with the size of the damage as well as the distance between the measuring point and the damage.

In the considered case of the leaf spring, the so-called zero-strain direction (which was initially derived by Schagerl et al. [9] for thin-walled structures) is of particular interest. This direction represents the direction in which no longitudinal strain is present within the undamaged reference state. The simplest way to illustrate zero-strain direction is to examine a plate-strip under unidirectional load, as shown in Fig. 1. The applied load leads to a high tensile strain in the x_1-direction while transverse contraction leads to a small negative strain in the x_2-direction. If the direction of the strain measurement is rotated by an angle β with respect to the x_1-direction, there is a certain angle $\beta_{1,2}$ where both effects cancel each other out. In this direction there is no longitudinal strain under the given load. In the considered case of the plate-strip, this zero-strain direction can be easily derived analytically. The longitudinal strain $\tilde{\varepsilon}_{11}$ in arbitrary direction β is dependent on the strain state of the x_1-x_2-plane:

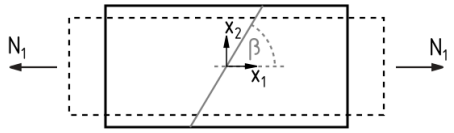

Fig. 1. Illustration of the zero-strain direction considering a plate-strip under unidirectional loading [5].

$$\tilde{\varepsilon}_{11} = \frac{\varepsilon_{11}+\varepsilon_{22}}{2} + \frac{\varepsilon_{11}-\varepsilon_{22}}{2} cos(2\beta) + \varepsilon_{12}\, sin(2\beta) \qquad (1)$$

In case of the considered load case and the given coordinate system, there is no shear strain ε_{12} present and thus, the equation can be rewritten as:

$$cos(2\beta) = \frac{\varepsilon_{11}+\varepsilon_{22}}{\varepsilon_{22}-\varepsilon_{11}} \qquad (2)$$

Using the definition of the Poisson's ratio $\varepsilon_{22} = -\nu_{12}\varepsilon_{11}$, the zero-strain direction is derived as:

$$\beta_{1,2} = \pm\frac{1}{2} arccos\left(\frac{\nu_{12}-1}{\nu_{12}+1}\right) \qquad (3)$$

Equation (3) shows that the zero-strain direction in the given case is only dependent on the Poisson's ratio ν_{12}. The height of the applied load has no influence on the zero-strain direction. So if a sensor, such as a strain gauge or FOS, is applied in this direction, it will measure zero in its initial state. However, if there is damage, then the load must be redirected around the damage (see Fig. 2) and as a consequence significant shear strains ε_{12} occur. These now lead to a measurable deviation from zero and thus indicate the damage.

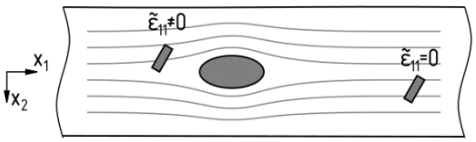

Fig. 2. Influence of the damage (grey ellipse) on the stress state illustrated by the principal stress direction (grey lines) [7].

The previously presented example of the plate-strip under unidirectional load is directly transferable to the leaf spring. If the leaf spring is imagined as being divided into a number of layers, then each of these is subjected to a unidirectional load in its plane (tensile or compressive, depending on the position relative to the neutral axis). If the strain in zero-strain direction is to be monitored in such a plane, then a meander-shaped sensor layout for an FOS

is obtained [2,5]. As shown in Fig. 3, it is characterised by several measuring sections in zero-strain direction (red lines) for damage monitoring. In between, the FOS is deflected with a radius. Measuring points in the longitudinal direction (blue dots) within the radius can also be used for load monitoring. Thus, a single meander-shaped FOS enables SHM and loads monitoring. A more detailed description of this sensor layout alongside of the simulation of a virtual sensor was given previous publications [2,5].

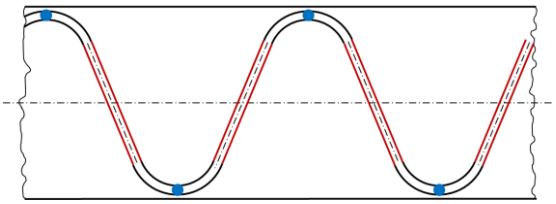

Fig. 3. Illustration of the zero-strain direction considering a plate-strip under unidirectional loading [5].

3 Test setup

The leaf spring was tested in a close-to-application setup using the actual mountings to the vehicle frame within the test setup as shown in Fig. 4. The mountings represent a typical fixed (right) and sliding (left) support. The load application was simplified, using a simple stamp instead of the actual centre clamping. An inclined surface was considered for the stamp in order to match the surface of the leaf spring and to provide a distributed loading over the whole stamp.

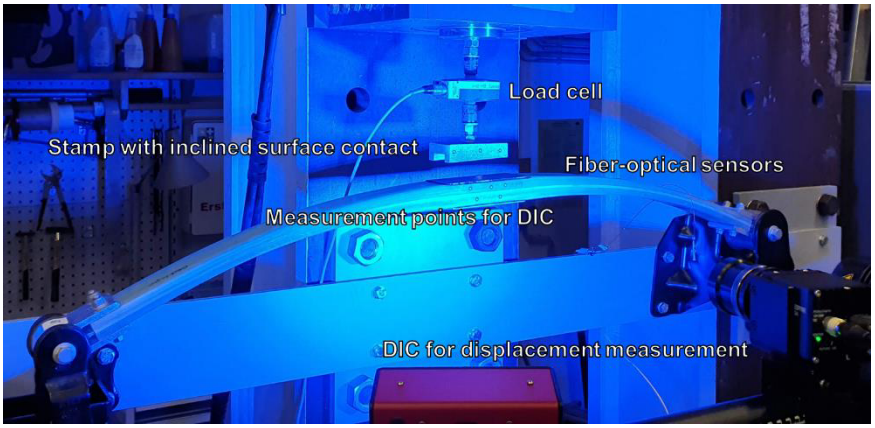

Fig. 4. Test setup using the actual vehicle mountings an DIC.

The applied load was measured using a load cell which was integrated between the servo-hydraulic piston and the stamp, while the centre displacement was monitored using Digital Image Correlation (DIC). Three quasi-static load levels were considered within the test campaign:

- 1650 N, representing the weight of an empty vehicle.
- 6000 N
- 12300 N, representing the design load of the leaf spring

Even though one FOS would have been sufficient, two FOS were integrated into each leaf spring to allow for fail-safety during the test. The FOS were integrated at 25% and 75% of the cross-section height. This position represents a compromise between sensitivity for

loads monitoring (a position more outwards would lead to higher readings) and the protection of the sensor from possible impacts in service. The actual sensor layout for the demonstrator tests is shown in Fig. 5 by the red line. The grey area on the left symbolises the connection to the eye, while the grey area on the right represents the load application area.

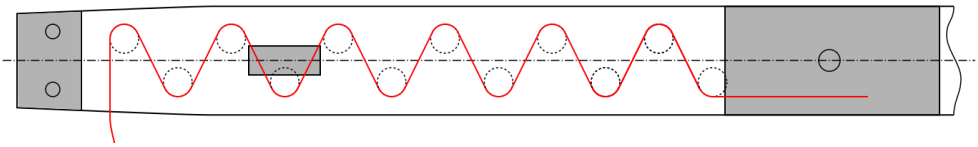

Fig. 5. Sensor layout (red line) within the leaf spring and position of the artificial delamination (grey rectangle).

As FOS, a polyimide coated glass fibre with 125 µm cladding diameter and 9 µm core diameter was used. The FOS was evaluated using OFDR to measure a quasi-continuous strain distribution. To enable simple sensor integration, the sensor fibre was stitched via tailored fibre placement (TFP) onto a carrier fleece (see Fig. 6) which then was inserted at the desired position between the layers of the hosting prepreg material.

Fig. 6. FOS stitched to a carrier fleece using TFP.

In total eleven leaf springs were tested: eight of them were undamaged and three had an artificial delamination which was introduced by a peel ply in between the layers. The position of the artificial delamination is shown in Fig. 5 by the small grey rectangle.

4 Test results and discussion

All eleven leaf springs were tested at three load levels (approx. 1650 N, 6000 N, 12300 N). At each load level, the load was held for a few minutes to allow settlement and creep effects to subside. The deformed leaf spring at design load (12300 N) is shown in Fig. 7. All tested leaf spring showed an almost linear behaviour up to design load and there was only little scatter regarding the stiffness. This indicates that the artificial damage has very little influence on the structure. Neither was the stiffness noticeably affected, nor did the damage lead to non-linear damage or even failure.

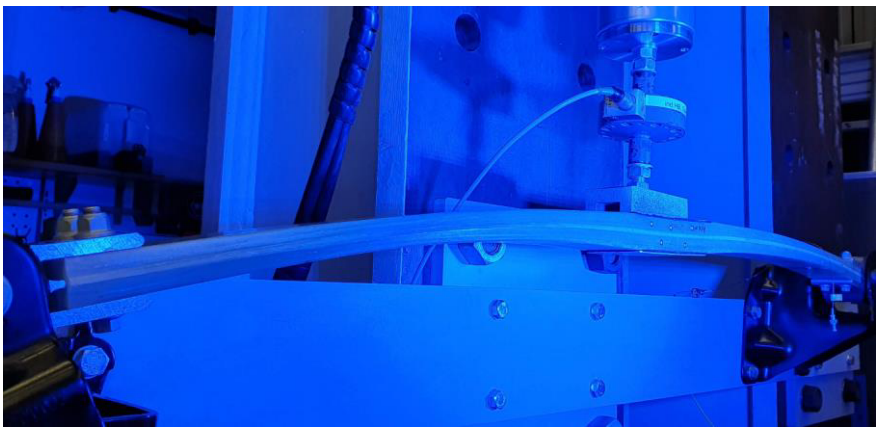

Fig. 7. Deformed leaf spring at design load (12300 N).

Fig. 8 shows an example of the strain measured by the FOS on an undamaged leaf spring under a load of 1730 N (note: due to the manual load control, the curb load was slightly exceeded). The characteristic strain curve can be easily recognised: passages with almost zero strain where the FOS runs in zero-strain direction and deflections with very high strain where the FOS is redirected in the radius and thus the strain is measured in the longitudinal direction. The peaks in the curve demonstrate that the sensor layout enables direct loads monitoring. Starting from the bearing, the measured strain increases towards the load application, analogous to the increase of the acting bending moment. In addition, a general deviation of the strain in the actual zero-strain direction can be observed. This indicates a small difference from the theoretical to the practical zero-strain direction. It should be noted that the Poisson's ratio as a determining factor cannot be exactly pre-determined and is also subjected to a small scatter. Also some scatter within the strain signal becomes evident.

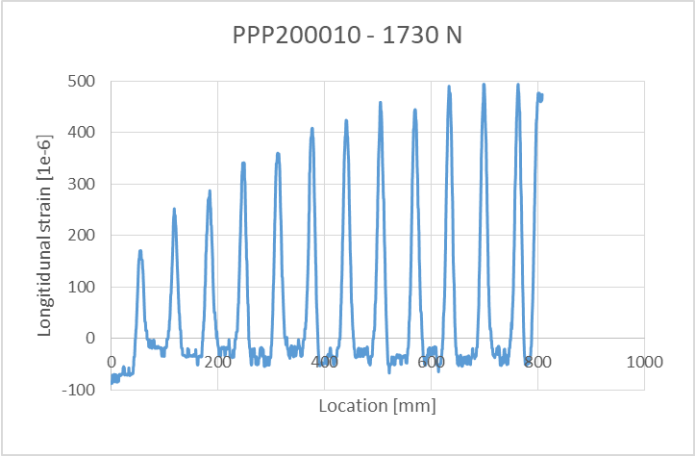

Fig. 8. Strain measurement of a single FOS of an undamaged leaf spring at curb load.

Fig. 9 shows the measured elongation of the same leaf spring at design load. The basic strain curve is identical. However, some artefacts can be seen which indicate a false and clearly excessive strain. The number of artefacts increased when the loading was repeated or increased. This indicates that micro-damages occurred in the FOS, which led to additional scattering and thus falsified the measurement signal.

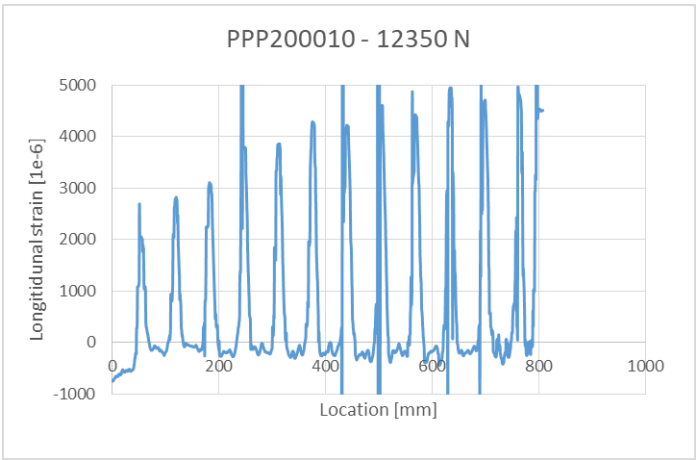

Fig. 9. Strain measurement of a single FOS of an undamaged leaf spring at design load.

The influence of the damage on the strain measured by the FOS is shown in Fig. 10. Here the elongation is plotted for two damaged leaf springs (18 and 19) compared to two undamaged leaf springs (05 and 10) under curb load. The diagram clearly shows that the scatter hinders an exact evaluation of the signal and assessment of the damage. However, it can be clearly seen that the damage in the range of 200 mm led to a significant deviation of the measured strain. The damage could thus be reliably detected and localised.

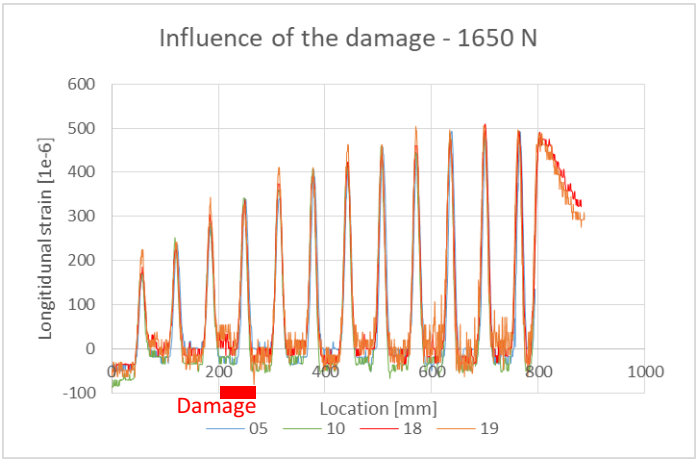

Fig. 10. Strain measurement of two damaged leaf springs (18 and 19) compared to two undamaged leaf springs (05 and 10).

5 Conclusion

This paper demonstrates the use of a meander-shaped sensor layout to monitor a GFRP leaf spring in combination with strain in zero-strain direction as a structural damage indicator. Using the proposed sensor layout, a single FOS can comprehensively monitor the complete leaf spring. The measuring points in the longitudinal direction show the profile of the resulting bending moment very well and thus provide direct information about the applied load. The monitoring of a mixed bending load would also be theoretically possible. The paths orientated in the zero-strain direction reliably detect the presence of damage. If there is

a clear deviation of the strain from the expected zero-value, this can be directly attributed to the damage. Due to the OFDR method, a quasi-continuous measurement was achieved which easily enables damage localization (level 2 monitoring according to Rytter). However, the relatively strong noise in zero-strain direction hinders an exact evaluation and thus an assessment of the damage. In addition, the sensor is prone to micro-damage when high loads are applied. This is a behaviour that was not expected and was only observed in the previous coupon tests at significantly higher loads [6].

It should be noted that during the test campaign many sensors could not or only partially be evaluated due to internal damage. Overall, 55% of the sensors were intact at the begin of the test campaign. It is assumed that the harsh production environment of the series production with its high process forces led to these sensor losses. It also seems likely that the preliminary damage was introduced here, which later led to the accumulation of micro-damage and thus to the described measurement artefacts. In future work, a closer look at the process forces and their influence on sensor damage is planned. In addition, a change from OFDR to FGB sensors is of interest. The layout loses its quasi-continuous measurement, but at the same time the influence of the measurement noise decreases when using FBGs.

This research was conducted within the framework of the project “Sensor Integration in Glass-Fiber Reinforced Plastics Leaf Springs for Structural Health Monitoring” (FA-0222). The authors are grateful to the Ford Motor Company for funding.

References

1. A. Rytter. Vibration Based Inspection of Civil Engineering Structures. PhD thesis. Aalborg, Denmark: Aalborg University (1993)
2. A. Preisler. Damage Detection and Assessment Based on Structural Damage Indicators. PhD thesis. Aachen, Germany: RWTH Aachen University (2020)
3. K. Peters. Fibre-optic Sensor Principles. In: Encyclopaedia of Structural Health Monitoring. Ed. by C. Boller, F.-K. Chang, Y. Fujino (2009)
4. A. Barrias, J.R. Cassas, S. Villalba. A Review of Distributed Optical Fiber Sensors for Civil Engineering Applications. In: Sensors 16, 1 (2016)
5. A. Preisler, F. Wolf-Monheim, A. Dafnis, K.-U. Schröder, P. van der Jagt, W. David, P. Zandbergen. Faseroptische Schadensüberwachung von GFK-Blattfedern mittels struktureller Schadensindikatoren. In: Smarte Strukturen und Systeme – Tagungsband des 4SMARTS-Symposiums (2019)
6. A. Preisler, F. Wolf-Monheim, D. Kaiser, R. Wojtczyk, A. Dafnis, K.-U. Schröder, W. David, P. Zandbergen. Integration and evaluation of a meander-shaped fibre-optical sensor in GFRP coupons. In: 10th EASN International Conference on "Innovation in Aviation & Space to the Satisfaction of the European Citizens (2021)
7. A. Preisler, K.-U. Schröder, M. Schagerl. Intrinsic Damage Assessment of Beam Structures Based on Structural Damage Indicators. In: American Journal of Engineering Research 7, 6 (2018)
8. A. Preisler, Z. Sadeghi, K.-U. Schröder. Monitoring of Fatigue Damages in Adhesively Bonded Joints. In: Proceedings of the 6th ECCOMAS Thematic Conference on the Mechanical Response of Composites (2017)
9. M. Schagerl, C. Viechtbauer, M. Schaberger. Optimal Placement of Fiber Optical Sensors along Zero-strain Trajectories to Detect Damages in Thin-walled Structures with Highest Sensitivity. In: Structural Health Monitoring – System Reliability for Verification and Implementation (2015)